Genetic variation in EEG activity during sleep in inbred mice

PAUL FRANKEN, ALAIN MALAFOSSE, AND MEHDI TAFTI
Biochemistry and Neurophysiology Unit, Department of Psychiatry, University of Geneva, CH-1225 Geneva, Switzerland

Franken, Paul, Alain Malafosse, and Mehdi Tafti. Genetic variation in EEG activity during sleep in inbred mice. *Am. J. Physiol.* 275 (*Regulatory Integrative Comp. Physiol.* 44): R1127–R1137, 1998.—The genetic variation in spontaneous rhythmic electroencephalographic (EEG) activity was assessed by the quantitative analysis of the EEG in six inbred mice strains. Mean spectral EEG profiles (0–25 Hz) over 24 h were obtained for paradoxical sleep (PS), slow-wave sleep (SWS), and wakefulness. A highly significant genotype-specific variation was found for theta peak frequency during both PS and SWS, which strongly suggests the presence of a gene with a major effect. The strain distribution of theta peak frequency during exploratory behavior differed from that during sleep. In SWS, the relative contributions of delta (1–4 Hz) and sigma (11–15) power to the EEG varied with genotype and power in both frequency bands was negatively correlated. In addition, the EEG dynamics at state transitions were analyzed with a 4-s resolution. The onset of PS, but not that of wakefulness, was preceded by a pronounced peak in high-frequency (>11 Hz) power. These findings are discussed in terms of the neurophysiological mechanisms underlying rhythm generation and their control and modulation by the brain stem reticular-activating system.

slow-wave sleep; paradoxical sleep; exploratory behavior; electroencephalogram spectral analysis; delta oscillations; theta oscillations; sigma oscillations; behavioral state transitions

RHYTHMIC ACTIVITY is one of the striking hallmarks of the central nervous system. Various behavioral states and brain regions are associated with oscillatory activity with frequencies ranging from <1 to >40 Hz and a spatial coherence ranging from localized clusters of neurons to the entire cerebral cortex (31, 34). Based on the electroencephalogram (EEG) characteristics, mammalian behaviors can be classified as wakefulness, paradoxical sleep (PS), or slow-wave sleep (SWS). SWS is characterized by a widespread synchronous activity in the delta (1–4 Hz)-frequency range and by spindle oscillations in the sigma (11–15 Hz) range. The structures implicated in the generation of these two mutually exclusive rhythms include the thalamus and the entire cerebral cortex (32). PS is characterized by theta oscillations (4–12 Hz) that can be observed in several regions of the limbic system, including the septum where it is thought to be generated (42, 43). Wakefulness encompasses a variety of behaviors, each with their characteristic EEG pattern. These vary from drowsiness, during which delta waves can intrude, to exploratory behavior characterized by theta waves and from quiet wakefulness with eyes closed characterized by alpha waves (8–13 Hz) to activity during the attention process characterized by gamma waves (>20 Hz; "40-Hz" oscillations). Both PS and wakefulness are considered activated brain states that share common EEG characteristics, such as the absence of delta and spindle activity and the presence of coherent gamma activity (24). The suppression of delta and spindle activity is due to the excitatory action of several ascending activating systems projecting to the thalamus and cortex (33). These systems can increase their activity during SWS in anticipation of arousal or PS, indicating their active role in the initiation and maintenance of these states.

Despite the progress in our understanding of the neurophysiological mechanisms underlying the generation of rhythmic brain activity, their genetic determinants remain mostly unknown. A number of studies have demonstrated that EEG characteristics are among the most heritable traits in humans (3). In most of these studies, alpha and beta rhythms in the waking EEG were compared in monozygotic (MZ) twins and for some rare alpha- and beta-EEG variants a simple, autosomal dominant mode of inheritance was found (30, 45). With quantitative EEG analysis, an overlap of 84% between spectral profiles was found within MZ pairs (4). Although several studies assessed genetic determinants of the amount and architecture of sleep (in humans, e.g., Refs. 23, 44, 46; in inbred mice, e.g., Refs. 35, 39) and many studies addressed the genetic determinants of pathological EEG activity (e.g., seizure activity), systematic and quantitative studies assessing the genetic contribution to normal rhythmic brain activity across behavioral states are lacking in mammals, especially in the mouse, which is the mammalian model of choice for the genetic study of complex behaviors and higher brain functions. With the recent introduction of gene targeting and transgenesis techniques, in an increasing number of studies sleep and EEG in mice lacking some candidate gene function are being recorded. However, in addition to the many drawbacks related to the use of these "knockout" mice (15), the "normal" (genetic) range of EEG variables across several inbred strains of mice has not yet been characterized. The aim of the present study was therefore twofold. A first aim was to characterize the EEG of mice during wakefulness, PS, and SWS and its spectral dynamics at transitions between behavioral states. A second aim was to estimate the genetic variability of these characteristics by comparing six commonly used inbred strains. Because, after at least 20 generations of

The costs of publication of this article were defrayed in part by the payment of page charges. The article must therefore be hereby marked "*advertisement*" in accordance with 18 U.S.C. Section 1734 solely to indicate this fact.

sibling mating, inbred strains can be considered as clones of fully homozygous and genetically identical individuals, it is possible to estimate both the genetic (between-strain variability) and environmental (within-strain variability) contribution to a phenotype. This study can provide a basis for the integration of neurophysiological and genetic approaches to clarify the mechanisms underlying rhythmic brain activity during sleep.

MATERIALS AND METHODS

Animals and housing conditions. Adult male mice from six inbred strains were used in this study (n = 7/strain). Five strains [AKR/J (AK), BALB/cByJ (C), C57BL/6J (B6), C57BR/6J (BR), DBA/2J (D2)] were purchased from Jackson Laboratory. The sixth strain, 129/Ola (129), was bred locally. The age at the day of recording ranged from 71 to 87 days (range of mean age/strain: BR, 75; B6, 84 days), and body weight ranged from 24 to 35 g (range of mean weight/strain: B6, 27; AK, 30 g). Mice were individually housed in polycarbonate cages (31 × 18 × 18 cm) in an experimental room with an ambient temperature that varied between 23 and 25°C under a 12:12-h light-dark cycle (lights on at 0800; 90 lx, fluorescent tube 40 W). Food and water were available ad libitum. Animals were kept under these conditions for at least 18 days before the experiment.

Surgery. EEG and electromyogram (EMG) electrodes were implanted under deep pentobarbital sodium anesthesia (65–75 mg/kg ip depending on strain). Two gold-plated screws (diameter 1.1 mm) served as EEG electrodes and were screwed through the skull over the right cerebral hemisphere (frontal: 1.7 mm lateral to midline, 1.5 mm anterior to bregma; parietal: 1.7 mm lateral to midline, 1.0 mm anterior to lambda). Two other screws were implanted at the same coordinates over the left hemisphere and were used as anchor screws. Two insulated stainless steel wires served as EMG electrodes and were inserted between two neck muscles. The electrodes, which were soldered to recording leads before implantation, and the anchor screws were cemented to the skull. The recording leads were connected to a swivel contact and animals were allowed 10–14 days of recovery from surgery and habituation before the experiment.

Experimental protocol and data acquisition. Eight to sixteen animals were recorded simultaneously in one session. Two to four strains were included in each session in an attempt to equally distribute the nonspecific (environmental) variation over strains. In each session, EEG and EMG signals were recorded continuously for four consecutive 24-h periods. Data from the second 24-h period, starting at lights on, and 5 min of the third 24-h period (exploratory behavior; see below) are presented here. The analog EEG and EMG signals were amplified (2,000×) and filtered. High-pass filter was set at 0.016 Hz (−3 dB point), and low-pass filters were set at 45 Hz (−3 dB point) and 128 Hz (−40 dB point). Signals were then analog-to-digital converted at 256 Hz, digitally filtered (FIR filters; EEG: low pass 25 Hz; EMG: band pass 20–50 Hz), and stored with a 128-Hz resolution. The EEG signal was subjected to a fast Fourier transformation (FFT) analysis, yielding power spectra between 0.125 and 25.125 Hz, with a 0.25-Hz frequency and a 4-s time resolution. The EMG was full-wave rectified and integrated over 4-s epochs. These analyses were performed online and the results were stored on magneto-optical disks. Acquisition hard- and software were purchased from Geltron Apparatebau and the Institute of Pharmacology, University of Zürich, respectively (both located in Zürich, Switzerland).

Determination of behavioral states. Offline, the animals' behavior was classified as PS, SWS, or wakefulness, on the basis of the EEG and EMG. The EEG during PS was characterized by a regular, low-amplitude theta (5–9 Hz) rhythm (Fig. 1) and a low EMG. During SWS, the EEG amplitude was larger and dominated by both delta (1–4 Hz)- and theta-frequency components (Fig. 1) and the EMG was low. Wakefulness was characterized by a higher and variable EMG and a low-amplitude EEG to which both slower (delta during drowsiness) and faster (theta during exploratory behavior; Fig. 1) frequency components could contribute. States were determined for consecutive 4-s epochs by the visual inspection of the EEG and EMG signals, which were displayed on a personal computer screen together with 4-s values for integrated EMG and EEG power in delta and theta. Epochs with artifacts in the EEG were identified and omitted from subsequent analysis and amounted to 2.7 ± 0.4% (mean ± SE, n = 42) of total recording time (24 h). In addition, the EEG spectrum during exploratory behavior was studied. The analysis was performed over the first 5 min after a cage change, 3 h after lights-on during the third 24-h recording period. During this period all animals were engaged in exploratory behavior.

EEG spectral profiles of the behavioral states. For each behavioral state and animal, a mean EEG spectrum was obtained by averaging the spectra of all 4-s epochs of a state in the 24-h recording period. Epochs of which one or both of the adjacent epochs were of a different behavioral state or contained an artifact were not included. This criterion was used to reduce the relative contribution of 4-s epochs containing more than one behavioral state. A total of 9,975 ± 259 4-s epochs met this criterion for wakefulness, 6,469 ± 200 for SWS, and 809 ± 31 for PS (mean ± SE; n = 42). Thus 80% of total recording time was used. Two analyses were performed on the EEG spectra. First, spectra between behavioral states within and between strains were compared. For this analysis, differences in the absolute power between individuals were accounted for as follows. Power density in each frequency bin and for each state was expressed as a percentage of the mean total EEG power over all frequency bins and states. This reference value was weighted in such a way that within each animal each state contributed with an equal number of 4-s epochs to the total EEG power over all states. This was necessary, because the time spent in each state varied with strain (Table 1). Second, spectral profiles of each behavioral state were compared among genotypes. For this analysis, EEG power density in each frequency bin was expressed as a percentage of the total EEG power for that behavioral state. In this way, variations in absolute power density within each

Table 1. *Time spent in each behavioral state*

Mouse Strain	W	SWS	PS
AK	52.0 ± 0.9*	42.8 ± 0.7†	5.0 ± 0.2*‡
C	56.1 ± 1.0*‡	38.7 ± 0.9†‡	5.2 ± 0.2*†‡
B6	59.4 ± 1.8†‡	35.6 ± 1.5*‡	4.8 ± 0.3*
BR	60.1 ± 0.9†‡	33.8 ± 1.3*‡	6.0 ± 0.6†‡
D2	63.6 ± 1.7†	31.3 ± 1.8*	4.8 ± 0.1*
129	59.3 ± 3.1†‡	34.6 ± 3.1*‡	6.1 ± 0.3†

Values are mean percentages ± SE (n = 7) of artifact-free recording time for amount of wakefulness (W), slow-wave sleep (SWS), and paradoxical sleep (PS). Time spent in each behavioral states varied among strains (1-way ANOVA: W, $P < 0.005$; SWS, $P < 0.001$; PS, $P < 0.05$). AK, AKR/J; C, BALB/cByJ; B6, C57BL/6J; BR, C57BR/6J; D2, DBA/2J; 129, 129/Ola mice. Mean strain values that significantly differed from other strains are indicated with a different symbol (t-test; $P < 0.05$).

state and animal were accounted for. Because the predominant theta frequency depended on behavior (Figs. 1–4), the frequency range over which theta power was analyzed varied accordingly: SWS, 5.5–8.5 Hz; PS, 6.0–9.0 Hz; exploratory behavior, 7.0–10.0 Hz.

Distribution of peak frequency. The EEG spectral profiles of PS and exploratory behavior were dominated by one frequency component only, whereas that of SWS was characterized by two (Figs. 2 and 3). To determine the prevailing frequency of each of these components, the distribution of peak frequency was calculated. In each of the 4-s epochs selected for each behavioral state (see above), the frequency bin with the highest power density was counted. The number of counts per frequency bin was expressed relative to the total number of counts. Because in PS the distribution of peak frequency of the theta component was normally distributed for all 42 individuals, we assumed that the bimodal distribution in SWS could be approximated by the sum of two normal distributions, one underlying each frequency component. For each animal, the sum of the squared differences between the actual distribution of peak frequency and the sum of two normal distributions was minimized by systematically varying mean, variance, and amplitude of each normal distribution. The sum of the two amplitudes, and thus the sum of the two normal distributions, was set to one. The mean peak frequencies of the two distributions with which the best fit was obtained were used for further statistical analysis.

Spectral changes at behavioral state transitions. The EEG changes accompanying a change in behavioral state were analyzed by automatically selecting clear transitions from one behavioral state (*A*) to another (*B*). The selection criterion was as follows: eight or more consecutive 4-s epochs scored as *A* had to be immediately followed by eight or more consecutive 4-s epochs scored as *B*. A mean time course of the power spectrum was constructed by aligning all selected transitions with respect to the time between the last 4-s epoch scored as *A* and the first one scored as *B* (time = 0 min in Fig. 5). Power values were then averaged over corresponding 4-s epochs (first within individuals, then over individuals of each strain). Only values in epochs scored as *A* in the 2 min before or scored as *B* in the 2 min after the *A*-*B* transition were included in the analysis. Within individual transitions, values were expressed as a percentage of the mean power over the 4-s epochs scored as SWS in the 3 min before (SWS to wakefulness or to PS) or after a transition (wakefulness to SWS). This analysis was initially performed for all 0.25-Hz frequency bins between 0.125 and 25.125 Hz. On the basis of contour plots of EEG power density versus time and frequency, three representative frequency bands were selected in which changes in power density were similar and most pronounced but distinct from the other two bands: delta (1.5–4.0)-, theta (6.0–8.5)-, and a high-frequency (11.0–19.0 Hz) band, which included the spindle frequencies (11–15 Hz). Before averaging over frequency bins, power in each bin was expressed relative to the mean SWS power for that bin (see above) to avoid bins with a high absolute power density contributing more to the mean. The time course of peak frequency was analyzed at the SWS-PS transition and was determined by identifying the frequency bin in which power density was highest for a given 4-s epoch. Only data from epochs scored as SWS in the 2 min before or as PS in the 2 min after the transition were included in the analysis.

Statistics. All main effects of factors "strain," "behavioral state," and "time" at transition (see RESULTS) on EEG power density and peak frequency were analyzed by one- or two-way ANOVA. Whenever main effects reached significance levels ($P < 0.05$), post hoc two-sided *t*-tests, corrected for multiple pairwise comparisons, were performed to further evaluate differences between the levels of the factors analyzed.

RESULTS

The EEG did not only differ markedly among behavioral states but also among strains. This is illustrated in Fig. 1. The most salient EEG features were the regular theta rhythm during PS of which the frequency varied with genotype (e.g., AK vs. BR), the larger amplitude in SWS compared with PS and wakefulness, and the different relative contribution of slow (delta) and faster (theta) frequency components to the SWS EEG (e.g., D2 vs. C). Because the EEG during wakefulness was highly dependent on the animals' behavior, EEG samples are shown for exploratory behavior only. AK, B6, BR, and 129 displayed a very regular theta rhythm, whereas that of D2 and C was more irregular and intermingled with both slower and faster components. These observations were quantified by determining the spectral composition of the EEG by FFT analysis.

Spectral profiles of the behavioral states. Power density differed clearly among states and varied over a wide range of frequencies (Fig. 2). Apart from the obvious power differences in the delta- and theta-frequency bands, on which the discrimination into behavioral states was partly based, the contribution of higher-frequency components greatly differed. These state-dependent spectral differences were affected by genotype (Table 2*A*). The significant interaction in the range between 1.1 and 4.6 Hz were largely due to the low values in SWS for D2 (relative to the values in both PS and wakefulness) and the relatively large SWS values in AK (*t*-test, $P < 0.01$). Between 5.4 and 6.6 Hz, strain differences were due to the different theta peak frequency in PS (see below); PS values for AK and C were already high relative to values in SWS and wakefulness, because theta peaked at a lower frequency. The reverse was true in the lower frequencies of the 7.4- to 11.4-Hz range; here PS power for BR was still high relative to values in the other behavioral states because peak frequency in PS was highest for BR. In addition, in the higher frequencies of the 7.4- to 11.4-Hz range, both AK and D2 displayed high values in SWS relative to the other two states.

The effect of genotype on EEG was further analyzed within each behavioral state by expressing the EEG power density in each frequency bin as a percentage of the total EEG power for that state (data not shown, but shape of the spectra as in Fig. 2). In PS, the spectral profile was dominated by one component only (Fig. 2); power in the theta range (i.e., 16% of the frequency range analyzed) accounted for 54% of total power and differed among genotypes due to higher values in AK (Table 3). The SWS spectrum was characterized by important contributions of power in both delta- and theta-frequency ranges and a less important contribution of the sigma-frequency range (Fig. 2, Table 3). The relative contribution of delta and sigma power to the total EEG power in SWS was a function of genotype (Table 3). In contrast, theta power did not vary. Varia-

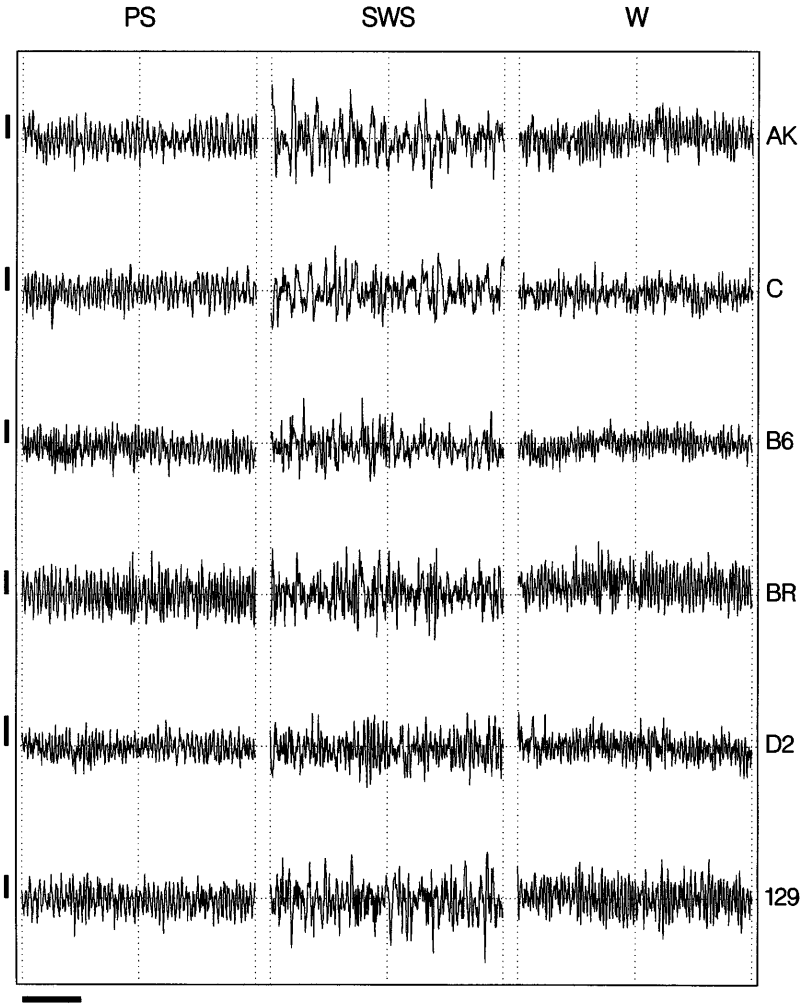

Fig. 1. Representative 8-s electroencephalogram (EEG) samples for paradoxical sleep (PS), slow-wave sleep (SWS), and wakefulness (W) from 1 animal of each inbred strain. SWS and PS samples were selected from the first 2 h of the light period. W samples were taken from the 5 min after a cage change when all animals were engaged in exploratory behavior. Horizontal bar, 2 s; vertical bars, 75 mV. Note the difference in frequency in PS [AKR/J (AK) vs. C57BR/6J (BR) mice] and W [BALB/cByJ (C) vs. BR mice] and the larger relative contribution of "slow waves" (<4 Hz) to the SWS EEG [AK vs. DBA/2J (D2)]. B6, C57BL/6J mice; 129, 129/Ola mice.

tions in delta and sigma power were negatively and significantly correlated ($r = -0.83$, $P < 0.001$, $n = 42$). Within strains, similar relationships were found but reached significance levels only for C ($P < 0.05$), B6, and 129 ($P < 0.01$, $n = 7$). Theta power did not significantly covary with delta or sigma power (theta vs. delta: $r = -0.22$, $P = 0.16$; theta vs. sigma: $r = -0.29$, $P = 0.07$, $n = 42$). Wakefulness was the least homogeneous behavioral state and encompassed a variety of behaviors, ranging from drowsiness to exploratory behavior, which were associated with different EEG patterns. This large variability is reflected by a low and broad spectral profile consisting of several frequency components mainly between 3 and 10 Hz (Fig. 2). During exploratory behavior all animals displayed a theta-dominated EEG (Figs. 1 and 3), which was the least regular for D2 and C. This observation is corroborated by a genotype-specific contribution of power in the theta range (Table 3).

Distribution of peak frequency. The EEG samples shown in Fig. 1 already indicate that the theta frequency in PS varied as a function of genotype. Analysis of the distribution of peak frequency revealed a segregation into three distinct groups (AK = C < D2 = 129 = B6 < BR, *t*-test, $P < 0.0001$) of which the individual values did not overlap (Fig. 4). This finding constitutes the most significant genotype-specific EEG difference in this study (1-way ANOVA, $F_{5,36} = 61.0$, $P = 1.4^{-16}$) Theta frequencies in PS were slightly but significantly higher (+0.20 Hz) in the 12-h dark or active period compared with the 12-h light period, but this difference was genotype independent (Table 2*B*).

The distribution of peak frequency in SWS showed a clear bimodal distribution in the lower frequencies (<9 Hz; Fig. 4) in five of the six strains (although not obvious from the mean distribution, the individual curves for 129 displayed bimodality as well). Analysis of the distribution of the peak frequency of the theta component in SWS showed a similar grouping as for PS, but due to a larger variability and relatively lower values for 129, the distinction between the slow and intermediate group was less clear (1-way ANOVA, $P < 0.0001$; AK = C = 129 < 129 = D2 = B6 < BR; *t*-test, $P < 0.005$) (Fig. 4). The theta frequency was lower in SWS compared with PS (−1.1 Hz), but again this difference was not affected by genotype (Table 2*C*). The delta component of the distribution of peak frequency varied less with genotype and reached significance levels only because of lower values for AK (1-way ANOVA, $P < 0.05$, t-test, $P < 0.05$) (Fig. 4).

The theta frequency during exploratory behavior also varied among genotypes (Table 3). However, because D2 now displayed the lowest theta frequency and AK no longer differed from B6, the genotype distribution of theta frequency during exploratory behavior clearly differed from that during sleep.

EEG changes at behavioral state transitions. In addition to the global EEG spectral profiles discussed above, we also analyzed the EEG dynamics at state transitions, in particular the transitions from wakefulness to SWS (W-SWS) and from SWS to PS (SWS-PS) or to wakefulness (SWS-W) (Fig. 5, SWS-W transition not shown). In general, as discussed above, power density was higher in SWS compared with PS and wakefulness, except for theta power in PS (Fig. 5, *middle*). Also confirmed with the transition analysis were the genotype-specific differences between power in SWS and W and between SWS and PS; e.g., the difference in delta power before and after the W-SWS transition was clearly smaller for D2 compared with AK (Fig. 5, *left*). However, of interest for this analysis is the timing of the changes in EEG power associated with the state changes. Therefore, the 2 min before and after each transition were analyzed separately and the power values in each period were expressed relative to the mean power in that period. Spectral dynamics were summarized by selecting three representative frequency bands: delta (1.5–4.0; Fig. 5, *left*)-, theta (6.0–8.5 Hz; Fig. 5, *middle*)-, and a high-frequency band (11.0–19.0 Hz; Fig. 5, *right*).

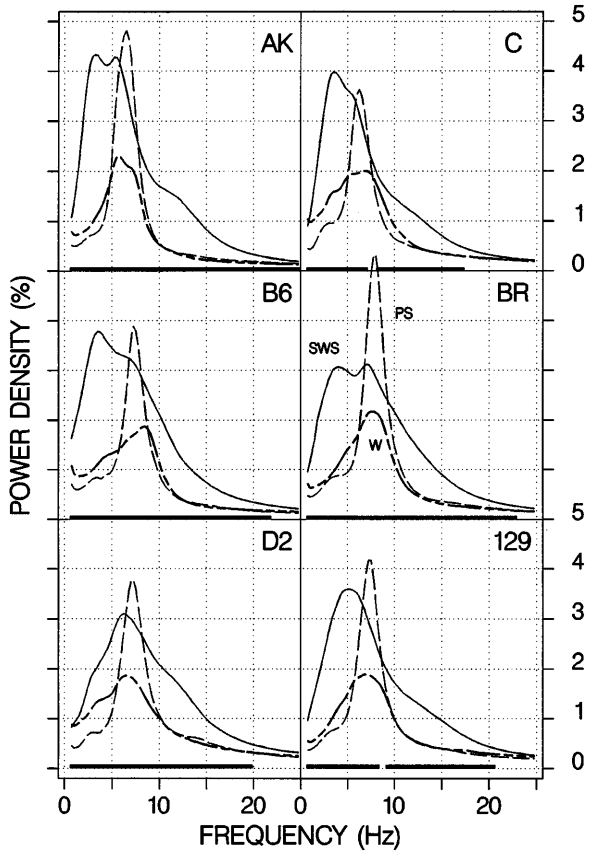

Fig. 2. Mean spectral profiles for SWS (solid lines), PS (short-dashed lines), and W (long-dashed lines). For 97 consecutive 0.25-Hz bins between 0.6 and 25.1 Hz, mean power density was calculated by averaging over all 4-s epochs scored as SWS, PS, or W in the 24-h recording period. All values were expressed as a percentage of mean total power for all frequencies and behavioral states (see MATERIALS AND METHODS). Within each panel, a thick horizontal line at the 0% level connects those frequency bins in which power density significantly varied among behavioral states (1-way ANOVA; factor "state" within each strain, $P < 0.01$, $n = 7$/strain).

Table 2. *Summary statistics*

Factor	*P*	EEG Frequency
	Spectral profiles	
A		
Strain	<0.01	0.6–25.1 Hz
State	<0.01	0.6–6.9, 7.1–25.1 Hz
Interaction	<0.01	1.1–4.6, 5.4–6.6, 7.4–11.4 Hz
	Theta peak frequency	
B		
Strain	<0.0001	
12-h Period	<0.0001	
Interaction	>0.5	
C		
Strain	<0.0001	
Sleep state	<0.0001	
Interaction	>0.2	
	Power at transitions	
D		
Strain	<0.0005	delta, theta, high frequency
Time	<0.0001	delta, theta, high frequency
Interaction	<0.0001	delta, theta, high frequency
E		
Strain	>0.6	delta, theta, high frequency
Time	<0.0001	delta, theta, high frequency
Interaction	<0.0001	delta, high frequency
	>0.1	theta
F		
Strain	>0.4	delta, theta, high frequency
Time	<0.0001	delta, theta, high frequency
Interaction	<0.0001	delta, theta, high frequency
	Peak frequency at transition	
G		
Strain	<0.0001	
Time	<0.0001	
Interaction	>0.9	

Significance levels (*P*) for the factors in the 2-way ANOVAs supporting the effects described in RESULTS, where they are referred to by characters (*A*–*G*).

Before the W-SWS transition, power in all frequencies remained constant and no significant strain differences were observed (Fig. 5). After the W-SWS transition, power increased rapidly in all frequencies, but the rate of increase was genotype and frequency dependent (Table 2*D*). In delta, the 100% level (mean delta power in SWS in the 3 min after the transition; Fig. 5) was reached first by D2 and last by C (Table 4). The time course of EEG power in the remaining two frequency bands was similar, and the time at which the 100% level was reached did not differ (difference between high-frequency and theta band: 1.0 ± 1.2 s; $P > 0.4$, paired *t*-test, $n = 42$) and was not affected by genotype (1-way ANOVA, factor strain, $P > 0.3$). However, the time at which power in the theta + high-frequency range reached 100% was a function of genotype (Ta-

Table 3. *Relative delta, theta, and sigma power in SWS, theta power in PS, and theta power and frequency in exploratory behavior*

Mouse Strain	SWS			PS	Exploratory Behavior	
	Delta	Theta	Sigma	Theta	Theta	Frequency
AK	26 ± 1*	26 ± 1	13 ± 0†‡	63 ± 1*	57 ± 1*	8.2 ± 0.1†‡
C	26 ± 2*	25 ± 1	13 ± 1‡	52 ± 2†	36 ± 2†	7.9 ± 0.2‡
B6	23 ± 1*†	27 ± 1	13 ± 1‡	54 ± 2†	54 ± 2*	8.7 ± 0.1*†
BR	19 ± 1†‡	26 ± 1	16 ± 1*†	55 ± 2†	52 ± 4*	8.9 ± 0.1*
D2	14 ± 1§	28 ± 1	18 ± 1*	50 ± 2†	32 ± 2†	7.9 ± 0.1‡
129	19 ± 2‡	27 ± 1	15 ± 1†‡	54 ± 2†	50 ± 2*	8.5 ± 0.2*†

Values are mean power in 3 frequency bands ± SE ($n = 7$) as a percentage of total electroencephalogram (EEG) power (=100%) in SWS, PS, and exploratory behavior, respectively, except for mean frequency during exploratory behavior, which is in Hz ($n = 7$). In SWS, delta (1.5–4.0 Hz) and sigma (11.0–15.0 Hz) power varied among strains (1-way ANOVA, $P < 0.01$), whereas theta (5.5–8.5 Hz) power did not. Theta power in PS (6.0–9.0 Hz) and during exploratory behavior (7.0–10.0 Hz) did vary among strains (1-way ANOVA; PS: $P < 0.01$; exploratory behavior: $P < 0.001$). Mean theta frequency during exploratory behavior varied among strains (1-way ANOVA, $P < 0.0001$). Mean strain values that significantly differed from other strains are indicated with a different symbol (*t*-test; EEG power: SWS, PS: $P < 0.05$; exploratory behavior: $P < 0.001$; EEG frequency in exploratory behavior: $P < 0.005$).

ble 4). For AK, C, BR, and D2, it rapidly increased and tended to initially overshoot the 100% level, whereas for B6 and 129 power slowly approached that level (e.g., AK vs. 129; Fig. 5). For B6, D2, and 129, the time at which the 100% level was reached did not differ between delta power and power in the theta + high-frequency range (Table 4).

The time course of delta and high-frequency EEG power during SWS before the SWS-PS transition varied with genotype (Table 2*E*). In the minute before PS onset, prominent and frequency-specific changes were observed (Fig. 5). First, power in the high-frequency range started to increase at −39 ± 2 s (*I*), directly followed by an increase in theta power (−34 ± 1 s; *II*). At −26 ± 1 s, delta power started to decrease (*III*), whereafter high-frequency power peaked (−16 ± 1 s; *IV*) and subsequently abruptly declined. Theta power peaked at PS onset (4 ± 2 s; *V*). This sequence was highly reproducible, and the timing of the five successive events significantly differed (paired *t*-test, $P < 0.0001$, $n = 42$; *II-I*: 5.2 ± 1.2; *III-II*: 7.7 ± 1.4; *IV-III*: 10.4 ± 0.9; *V-IV*: 11.9 ± 1.8 s) and some of these events were affected by genotype due to a delay in D2 (1-way ANOVA, factor strain: *events I, II, IV*: $P < 0.01$; *event III*: $P > 0.05$; *event V*: $P > 0.3$). Interestingly, these events were specific for the SWS-PS transition and were not observed at the SWS-W transition (data not shown), at which, to a large extent, the time course of EEG power was reversed to that at the W-SWS transition. Also after the transition, the time course of power within PS varied with genotype (Table 2*F*). First delta- and later high-frequency power reached a low and constant level after the transition (Fig. 5). However, due only to the relative high initial values for B6 (*t*-test, $P < 0.01$) in both frequency bands, the first three or four epochs varied among strains (Fig. 5). In the theta-frequency range, after reaching peak values at the transition, power decreased to values comparable to those in SWS. Except for AK, where theta power already decreased before PS onset (theta peaked at −13 ± 4 s) and, as a consequence, in the first four epochs, the relative values for AK (relative to all PS theta values) were lower compared with other strains (*t*-test, $P < 0.01$) (Fig. 5).

Peak frequency started to increase before PS onset (−32 ± 1 s; Fig. 6) and coincided with the start of the increase of theta power (see above). However, the time course of theta power and frequency clearly differed thereafter (Figs. 5 and 6). The changes in peak frequency were remarkably similar among strains (Table 2*G*) and, after correcting for the genotype differences in absolute frequency, genotype affected frequency only in occasional epochs before the transition, largely due to high relative values for D2 (*t*-test, $P < 0.01$) (Fig. 6).

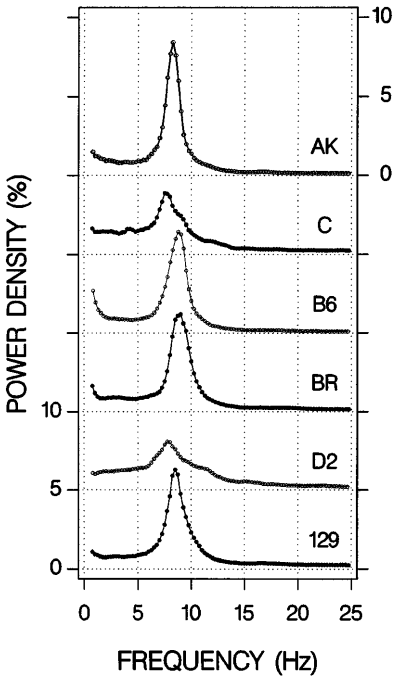

Fig. 3. Spectral EEG profiles for exploratory behavior are shown. For 97 consecutive 0.25-Hz bins between 0.6 and 25.1 Hz, mean power density was calculated by averaging over 75 4-s epochs after a cage change ($n = 7$/strain). All values were expressed as a percentage of mean total power. Filled and open circles are used in alternation to better distinguish between strains. In addition, the curves of each strain are offset by 10%.

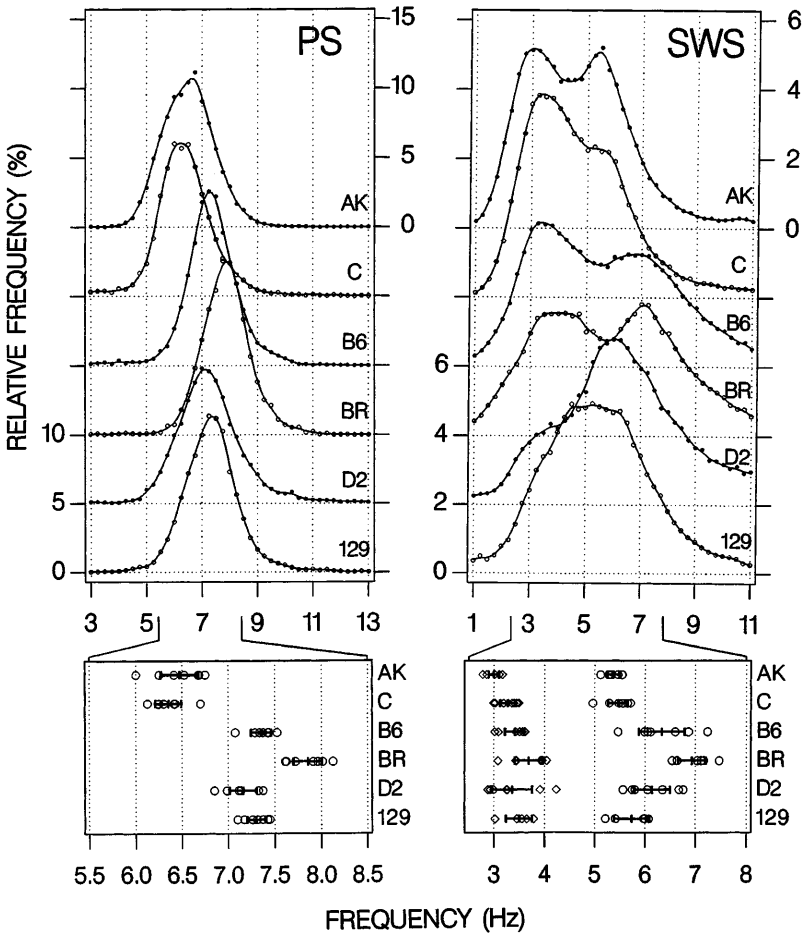

Fig. 4. *Top*: mean relative frequency distributions of peak frequency in PS (*left*) and SWS (*right*). In each 4-s epoch scored as PS or SWS, frequency bin in which power density was maximum was counted. Filled and open circles are used in alternation to better distinguish between strains (n = 7/strain). In addition, curves of each strain are offset by 5 (PS) or 2% (SWS). *Bottom*: for PS (*left*), mean peak frequency in each animal was based on individual frequency distributions. Individual peak frequencies are indicated by circles. Horizontal error bars connect ± 2 SEs. For SWS (*right*), frequency distribution was assumed to result from 2 distinct frequency components: 1 in the delta-frequency range, another in the theta range. To determine mean peak frequency of each component, the sum of 2 normal distributions was fitted to individual peak frequency distributions (see MATERIALS AND METHODS). ◇, ○, Individual peak frequencies in the delta and theta range, respectively.

DISCUSSION

Theta oscillations. The most prominent findings concern hippocampal theta. The predominant theta frequency in PS varied with genotype, and three clear groups could be distinguished. The highly significant effect of genotype, which could explain over 80% of the total variability among strains, strongly suggests the presence of a gene with a major effect on theta frequency. This gene may be involved in a variety of factors modulating theta frequency. First, differences in brain temperature might have contributed. Although 24-h temperature values for inbred mice are not available, inferences can be made from the relationship between temperature and theta frequency obtained in Djungarian hamsters. For this species a Q_{10} of 2.3 (i.e., with a 10°C increase, theta frequency increases 2.3-fold) was reported (10). With this value, the differences in theta frequency observed in the present study can be translated into expected temperature differences, which were compared with published values. The Q_{10} effect clearly underestimates the dark-light difference [observed: 0.2 Hz, expected: 0.3°C, reported for mice: 1°C (36)] and overestimates the PS-SWS difference [observed: 1.1 Hz, expected: 2.3°C, reported for Djungarian hamsters: 0.2°C (9)] and, most likely, also the expected temperature difference between strains [BR vs. C; observed: 1.5 Hz, expected: 2.5°C]. Therefore, temperature probably does not underlie the genotype-specific differences in theta frequency.

Second, the neurophysiological mechanisms regulating theta frequency might be genetically determined. Although several regions of the limbic system have the intrinsic capability to display theta-like activity, the septum is crucial for the expression of hippocampal theta in the intact animal (42, 43). The medial-septum/diagonal-band complex contains continuously bursting neurons that can be regarded as endogenous pacemakers. With increasing (nonoscillatory) excitatory input from the brain stem reticular formation (RF), the interburst interval of these pacemaker cells decreases and hippocampal theta frequency increases (6, 17, 25, 27, 41). Thus the excitatory input from the brain stem RF to the septum might vary with genotype, thereby affecting theta frequency. This could also explain, rather than temperature, the 1.1-Hz PS-SWS difference in theta frequency, because during SWS the excitatory input from the brain stem is decreased relative to PS (33). During exploratory behavior, the genotype-specific theta frequency distribution observed in sleep disappears. This suggests that only during sleep, when external sensory input and information processing is reduced, the background level of brain stem excitation is genotype dependent. The variation in theta frequency might, however, originate from any other mecha-

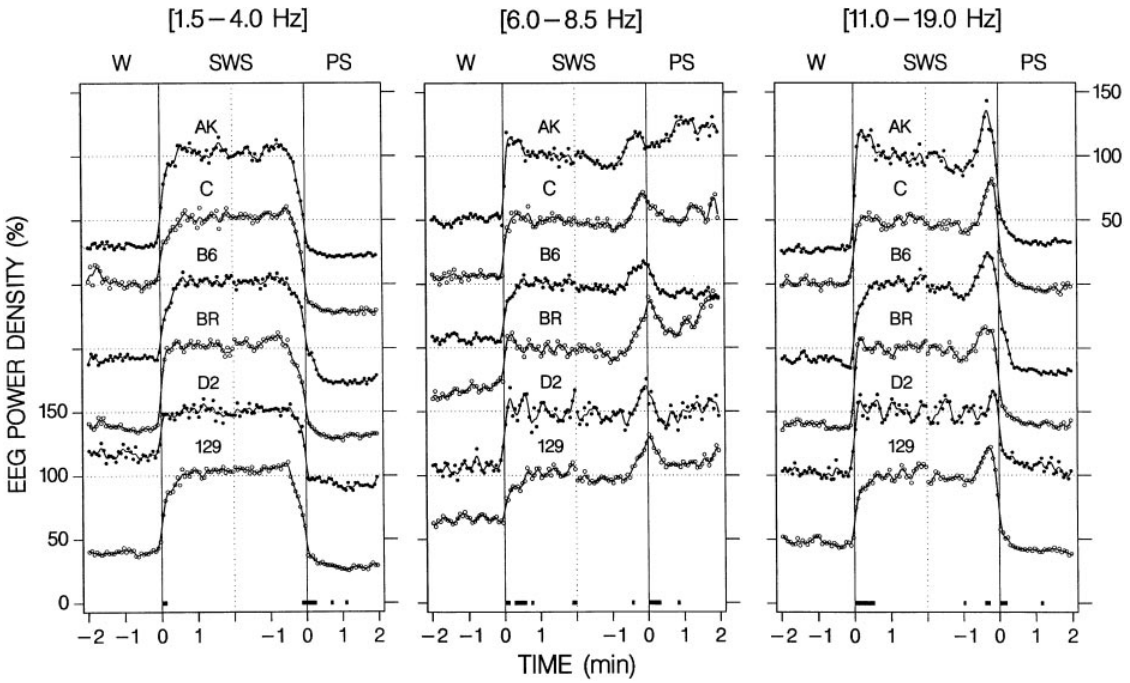

Fig. 5. Dynamics of EEG power at behavioral state transitions are shown. Time course of EEG power in the delta (1.5–4.0; *left*)- and theta (6.0–8.5 Hz; *middle*)-frequency range and in the range between 11.0 and 19.0 Hz (*right*) at the transition between W to SWS and from SWS to PS. All 4-s values were expressed as a percentage of the mean power of all 4-s epochs scored as SWS in the 3 min after the W-SWS transition or in the 3 min before the SWS-PS transition (100%). Only data for the 2 min before and after each transition are shown. Transitions at *time 0* are indicated by vertical solid lines. Filled and open circles are used in alternation to distinguish between subsequent strains. In addition, the curves for each strain are offset by 50%. Black horizontal bars at the bottom of each panel indicate 4-s epochs in which EEG power differed among strains (1-way ANOVA; $P < 0.01$; $n = 7$/strain). On average, 22.4 ± 1.9 W-SWS and 33.6 ± 3.9 SWS-PS transitions contributed to the mean transition curve in each animal ($n = 42$).

nisms implicated in its generation. Also, factors such as hippocampal size and anatomy, which vary among strains (2, 8, 29, 47), and PS "quality" (e.g., density of phasic events) might shape theta.

In the SWS EEG, clear theta activity was present and its relative contribution was as important as delta activity. Theta activity in SWS and PS seems to be of the same origin, because their frequencies share the same strain distribution in mice and the same Q_{10} in Djungarian hamsters, a rodent of comparable size (10).

Table 4. *Duration of the increase in EEG power after the W-SWS transitions*

Mouse Strain	Delta	Theta + High Frequency
AK	27 ± 4*†‡	7 ± 1‡
C	37 ± 3*	17 ± 3*†
B6	27 ± 5*†‡	24 ± 3*
BR	18 ± 4†‡	8 ± 1‡
D2	14 ± 2‡	13 ± 3†‡
129	34 ± 7*†	36 ± 2*

Mean time interval ± SE ($n = 7$) in s between SWS onset (0 s) and the time at which delta and theta + high-frequency power reached the mean level in SWS varied among strains (1-way ANOVA, delta: $P < 0.01$; theta + high-frequency band: $P < 0.0001$). Mean delta and theta + high-frequency power in SWS (100% level in Fig. 5) was calculated over the 3 min after SWS onset. Mean strain values that significantly differed from other strains are indicated with a different symbol (*t*-test, $P < 0.01$).

In contrast, the main delta frequency varied less and its strain distribution pattern did not parallel that of theta, which underscores that these two oscillations originate from different sources. In larger mammals, theta activity during SWS is only observed at the hippocampal level (e.g., 14, 22, 37). This might relate to cortical thickness [only 1 mm in mice (13)], because it determines the distance of the recording electrodes to the hippocampus and, possibly, also the relative contribution of slow waves to the SWS spectra, which can "mask" hippocampal theta. The latter effect was supported by the present study; the strain with the smallest cortex (D2) also had the smallest relative delta power, and the opposite was true for AK and C (28).

During exploratory behavior in mice, theta appeared fast and regular in some and slower and more irregular in others. Although all animals were engaged in continuous exploratory behavior during the recording period, slight differences in activity could have gone unnoticed and might have contributed to this difference. Especially spells of immobility, which were not quantified, can affect theta (40). Thus, even in a seemingly homogeneous behavior, subtle variations might result in pronounced EEG differences. This point can be of relevance in the study of genetic factors underlying learning and memory in which theta oscillations play an important role (7, 19, 26).

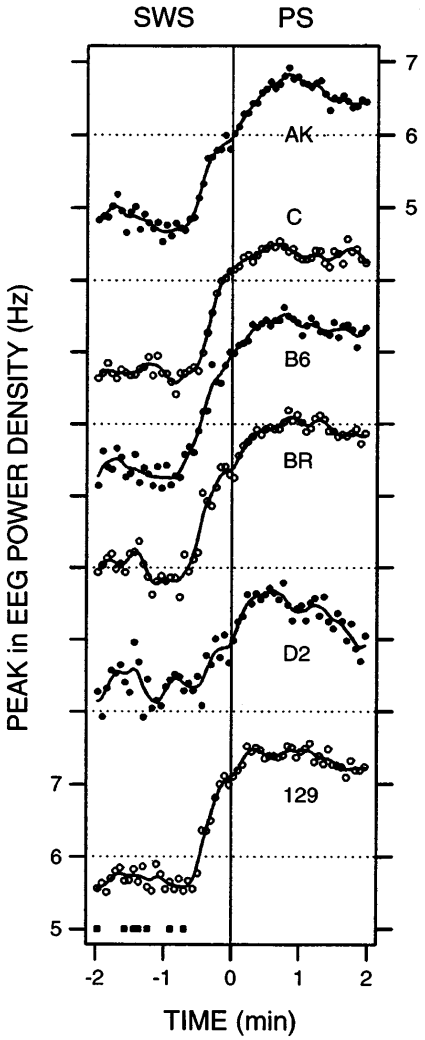

Fig. 6. Dynamics of peak frequency at the SWS-PS transition are shown. Frequency bin with the largest power density was determined in each 4-s epoch scored as SWS in the 2 min before the transition or as PS in the 2 min after the transition. Values were then averaged over transitions within each animal and over animals within each strain (34 transitions/animal, 7 animals/strain). Filled and open circles are used in alternation to distinguish between strains, and the curves for each strain are offset by 2 Hz. Horizontal bars at *bottom* indicate 4-s epochs in which peak frequency differed among strains (1-way ANOVA; $P < 0.01$; $n = 7$/strain) after expressing all values relative to the frequency at the transition to compensate for strain-specific differences in absolute frequency [1-way ANOVA, $P < 0.0001$; frequency at *time 0* (Hz); AK (5.9 ± 0.1) = C (6.1 ± 0.1) < D2 (6.8 ± 0.3) = B6 (7.0 ± 0.2) = 129 (7.1 ± 0.2) = BR (7.3 ± 0.1); *t*-test, $P < 0.05$, $n = 7$/strain].

Delta and spindle oscillations. Whereas theta oscillations are a network property of the limbic system, delta and spindle oscillations during SWS are generated in the thalamocortical network (32, 34). Synchronized EEG activity during SWS depends on a reduced excitatory input from the upper brain stem, posterior hypothalamus, and basal forebrain, which project to the entire cerebral cortex and thalamus (33). With decreasing excitatory input, the membrane potential of thalamocortical neurons hyperpolarizes and their firing patterns change from a tonic single-spike firing mode, characteristic of wakefulness and PS, to a rhythmic burst-pause pattern, characteristic of SWS. The interburst interval is a function of the degree of membrane hyperpolarization. At intermediate levels of hyperpolarization (i.e., at the early stages of sleep), spindles appear, which, as sleep progresses and thalamocortical neurons become more hyperpolarized, are replaced by slower, delta oscillations (34). This scenario, in which the presence of either oscillation precludes the presence of the other, is confirmed by observations at the EEG level in humans and cats (1, 11, 21). In the present study large genotype differences were found between the relative contribution of power in the delta and sigma range to the SWS EEG. Moreover, delta and sigma power were negatively correlated, which corroborates the hyperpolarization hypothesis and suggests a common genetic basis. Consistent with this hypothesis and our initial argument to account for differences in theta frequency, the delta-sigma balance might also be a function of a genotype-specific background level of brain stem excitation during SWS. If these levels remain relatively high, hyperpolarization of thalamocortical neurons is less pronounced, favoring the presence of spindles over delta oscillations. Alternatively, because the SWS amount was genotype dependent (Table 1), an increased sleep pressure, which augments delta and suppresses sigma power (5, 11, 21), might have played a role. However, this cannot explain the present results. On the contrary, the strain with the least amount of SWS (D2) displayed the lowest delta and highest sigma power, whereas AK and C, which slept the most, displayed the highest delta and lowest sigma power. It is more likely that D2, in general, has a higher level of excitability, reflected by less and more shallow (lower delta and higher sigma power) and more fragmented (data not shown) SWS.

EEG dynamics at state transitions. The analysis of the time course of EEG activity at state transitions might be instrumental in revealing genotype differences in the neurophysiological mechanisms underlying behavioral state control. At the W-SWS transition, important genotype differences were observed. High-frequency power, which included the spindle frequency range, peaked just after SWS onset in AK but not in B6 and 129. In these two strains the time course of high-frequency power resembled that of delta power. Delta power did not differ among these three strains. Thus, at least at the macroscopic level of the EEG, observations in some strains confirm data from other mammals (1, 11, 21) and support the hyperpolarization hypothesis, whereas in other strains the relationship between delta and sigma is less clear. Possible strain differences in thalamocortical synchronizing mechanisms, however, have to be addressed at a neuronal level. Other genotype differences concern the rate of increase of delta power after SWS onset, which might be related to a smaller W-SWS difference in delta power (D2) and to differences in sleep pressure (20).

The SWS-PS transition was invariably accompanied by a pronounced peak in high-frequency power and a decrease in delta power just before PS onset and a peak in theta power at PS onset. These changes in EEG

power were absent at the SWS-W transition and are in good agreement with observations in the rat (12, 38) and also confirm a previous, qualitative description of pre-PS events in C (16). The increase in high-frequency power before PS onset was not restricted to the spindle frequencies and started to increase well before delta power decreased. These observations contrast with the hyperpolarization hypothesis (see above), because a decrease in delta power should precede or at least coincide with an increase in high-frequency power. It has been suggested that this high-frequency spindle-like activity is of hippocampal origin and precedes the emergence of hippocampal theta before PS onset (18), as was the case in the present study. The same author described that in rats the frequency of this pre-PS theta activity is lower than during PS. In the present study, we confirmed this observation and, in addition, quantified the exact time course of theta frequency, which was remarkably similar among genotypes. Interestingly, although theta power and frequency started to increase simultaneously, theta power decreased after PS onset, whereas theta frequency further increased. Neurons from various brain stem structures, among which are the bulbar and medialpontine RF, and laterodorsal and pedunculopontine tegmental nuclei (LDT/PPT) increase their activity in anticipation of PS (33), which might contribute to the SWS-PS-specific EEG changes. For instance, neurons in the LDT/PPT are implicated in the generation of pontogenicolate-occipital (PGO) waves, which invariably herald PS onset. Other brain stem nuclei specifically decrease their activity before PS. For instance, unit activity in the raphe nuclei is inversely related to PGO waves and becomes virtually silent during PS (33). This decreased raphe activity might be permissive of the pre-PS appearance of theta and the further increase of theta frequency after PS onset, because it is the only brain stem structure where increased activity suppresses theta (41, 43). The interplay between the structures mentioned plays important roles in the initiation and maintenance of PS (33).

In conclusion, we have characterized and quantified several aspects of the sleep EEG of the most commonly used inbred mice and found that the rhythmic neuronal activity generated in the limbic system (hippocampal theta) during PS and SWS and thalamocortical network (delta waves and spindles) during SWS varies according to genotype. The relationship between delta and spindle oscillations and the time course of the EEG changes at the transitions between states are in good agreement with those obtained in other mammalian species. The results are discussed in terms of the neurophysiological mechanisms underlying the generation of these rhythms and a permissive and modulatory role for the brain stem reticular activating system. By characterizing those aspects of the sleep EEG that are under strong genetic control, this study constitutes a first step toward the identification of genes implicated in the generation and control of these sleep-related oscillations and will thus provide an important basis for further neurophysiological and genetic studies.

We thank Dr. Andrei Belousov for helpful discussions and Dr. Nihal Okaya for help with mathematical problems.

This study was supported by the Swiss National Science Foundation Grant 31.457513.95.

Address for reprint requests: P. Franken, HUG Belle-Idée, Dept. of Psychiatry, Biochemistry & Neurophysiology Unit, Chemin du Petit-Bel-Air 2, CH-1225 Chêne-Bourg, Switzerland.

Received 21 April 1998; accepted in final form 30 June 1998.

REFERENCES

1. **Aeschbach, D., and A. A. Borbély.** All-night dynamics of the human sleep EEG. *J. Sleep Res*. 2: 70–81, 1993.
2. **Barber, R. P., J. T. Vaughn, R. E. Wimer, and C. C. Wimer.** Genetically associated variations in the distribution of dendate granule cell synapses upon pyramidal cell dendrites in mouse hippocampus. *J. Comp. Neurol*. 156: 417–434, 1974.
3. **Beijsterveldt, C. E. M., and D. I. Boomsma.** Genetics of the human electroencephalogram (EEG) and event-related brain potentials (ERPs): a review. *Hum. Genet*. 94: 319–330, 1994.
4. **Beijsterveldt, C. E. M., P. C. M. Molenaar, E. J. C. Geus, and D. I. Boomsma.** Heritability of human brain functioning as assessed by electroencephalography. *Am. J. Genet*. 58: 562–573, 1996.
5. **Borbély, A. A., F. Baumann, D. Brandeis, I. Strauch, and D. Lehmann.** Sleep deprivation: effect on sleep stages and EEG power density in man. *Electroencephalogr. Clin. Neurophysiol*. 51: 483–493, 1981.
6. **Braznik, E. S., and O. S. Vinograda.** Control of the neuronal rhythmic bursts in the septal pacemaker of theta-rhythm: effects of anaesthetic and anticholinergic drugs. *Brain Res*. 380: 94–106, 1986.
7. **Buzsaki, G., L. S. Chen, and F. H. Gage.** Spatial organization of physiological activity in the hippocampal region: relevance to memory formation. *Prog. Brain Res*. 83: 257–268, 1990.
8. **Crusio, W. E., G. Genthner-Grimm, and H. Schwegler.** A quantitative-genetic analysis of hippocampal variation in the mouse. *J. Neurogenet*. 3: 203–214, 1986.
9. **Deboer, T., P. Franken, and I. Tobler.** Sleep and cortical temperature in the Djungarian hamster under baseline conditions and after sleep deprivation. *J. Comp. Physiol. [A]* 174: 145–155, 1994.
10. **Deboer, T., and I. Tobler.** Temperature dependence of EEG frequencies during natural hypothermia. *Brain Res*. 670: 153–156, 1995.
11. **Dijk, D.-J., B. Hayes, and C. A. Czeisler.** Dynamics of electroencephalographic sleep spindles and slow wave activity in men: effect of sleep deprivation. *Brain Res*. 626: 190–199, 1993.
12. **Franken, P., D.-J. Dijk, I. Tobler, and A. A. Borbély.** High-frequency components of the rat electrocorticogram are modulated by the vigilance states. *Neurosci. Lett*. 167: 89–92, 1994.
13. **Franklin, K. B. J., and G. Paxinos.** *The Mouse Brain in Stereotaxic Coordinates*. San Diego, CA: Academic, 1997.
14. **Gatztelu, J. M., M. Romero-Vives, V. Abraira, and E. Garcia-Austt.** Hippocampal EEG theta power density is similar during slow-wave sleep and paradoxical sleep. A long-term study in rats. *Neurosci. Lett*. 172: 31–34, 1994.
15. **Gerlai, R.** Gene-targeting studies of mammalian behavior: is it the mutation or the background genotype? *Trends Neurosci*. 19: 177–189, 1996.
16. **Glin, L., C. Arnaud, D. Berracochea, D. Galey, R. Jaffard, and C. Gottesmann.** The intermediate stage of sleep in mice. *Physiol. Behav*. 50: 951–953, 1991.
17. **Gogolak, G., H. Petschke, J. Sterc, and C. Stumpf.** Septum cell activity in the rabbit under reticular stimulation. *Brain Res*. 5: 508–510, 1967.
18. **Gottesmann, C.** The transition from slow-wave sleep to paradoxical sleep: evolving facts and concepts of the neurophysiological processes underlying the intermediate stage of sleep. *Neurosci. Biobehav. Rev*. 20: 367–387, 1996.
19. **Klimesch, W.** Memory processes, brain oscillations and EEG synchronization. *Int. J. Psychophysiol*. 24: 61–100, 1996.
20. **Lancel, M.** Cortical and subcortical EEG in relation to sleep-wake behavior in mammalian species. *Neuropsychobiology* 28: 154–159, 1993.

21. **Lancel, M., H. Riezen, and A. Glatt.** The time course of sigma activity and slow-wave activity during NREMS in cortical and thalamic EEG of the cat during baseline and after 12 hours of wakefulness. *Brain Res*. 596: 285–295, 1992.
22. **Lancel, M., H. Riezen, and A. Glatt.** Enhanced slow-wave activity within NREM sleep in the cortical and subcortical EEG of the cat after sleep deprivation. *Sleep* 15: 102–118, 1992.
23. **Linkowski, P., M. Kerkhofs, R. Hauspie, and J. Mendlewicz.** Genetic determinants of EEG sleep: a study in twins living apart. *Electroencephalogr. Clin. Neurophysiol*. 79: 114–118, 1991.
24. **Llinás, R. R., and D. Paré.** Of dreaming and wakefulness. *Neuroscience* 44: 521–535, 1991.
25. **McNaughton, N., and E. M. Sedgewick.** Reticular stimulation and hippocampal theta rhythm in rats: effects of drugs. *Neuroscience* 3: 629–632, 1978.
26. **O'Keefe, J.** Hippocampus, theta, and spatial memory. *Curr. Opin. Neurobiol*. 3: 917–924, 1993.
27. **Petschke, H., C. Stumpf, and G. Gogolak.** The significance of the rabbit's septum as a relay station between the midbrain reticular formation and the hippocampus. The control of hippocampus arousal activity by septum cells. *Electroencephalogr. Clin. Neurophysiol*. 14: 202–211, 1962.
28. **Roderick, T. H., R. E. Wimer, C. C. Wimer, and P. A. Schwartzkroin.** Genetic and phenotypic variation in weight of brain and spinal cord between inbred strain of mice. *Brain Res*. 64: 345–353, 1973.
29. **Schwegler, H., M. Boldyreva, R. Linke, J. Wu, K. Zilles, and W. E. Crusio.** Genetic variation in the morphology of the septo-hippocampal cholinergic and GABAergic systems in mice: II. Morpho-behavioral correlations. *Hippocampus* 6: 535–545, 1996.
30. **Steinlein, O., A. Anokhin, M. Yping, E. Schalt, and F. Vogel.** Localization of a gene for the human low-voltage EEG on 20q and genetic heterogeneity. *Genomics* 12: 69–73, 1992.
31. **Steriade, M., P. Gloor, R. R. Llinás, F. H. Lopes da Silva, and M.-M. Mesulam.** Basic mechanisms of cerebral rhythmic activities. *Electroencephalogr. Clin. Neurophysiol*. 76: 481–508, 1990.
32. **Steriade, M., and R. R. Llinás.** The functional states of the thalamus and the associated neuronal interplay. *Physiol. Rev*. 68: 649–742, 1988.
33. **Steriade, M., and R. W. McCarley.** *Brainstem Control of Wakefulness and Sleep*. New York, Plenum Press, 1990.
34. **Steriade, M., D. A. McCormick, and T. J. Sejnowski.** Thalamocortical oscillations in the sleeping and aroused brain. *Science* 262: 679–685, 1993.
35. **Tafti, M., P. Franken, K. Kitahama, A. Malafosse, M. Jouvet, and J.-L. Valatx.** Localization of candidate genomic regions influencing paradoxical sleep in mice. *Neuroreport* 8: 3755–3758, 1997.
36. **Tobler, I., T. Deboer, and M. Fisher.** Sleep and sleep regulation in normal and prion protein-deficient mice. *J. Neurosci*. 17: 1869–1879, 1997.
37. **Tobler, I., P. Franken, and R. Scherschlicht.** Sleep and EEG spectra in the rabbit under baseline conditions and following sleep deprivation. *Physiol. Behav*. 48: 121–129, 1990.
38. **Trachsel, L., I. Tobler, and A. A. Borbély.** Electroencephalogram analysis of non-rapid eye movement sleep in rats. *Am. J. Physiol*. 255 (*Regulatory Integrative Comp. Physiol*. 24): R27–R37, 1988.
39. **Valatx, J.-L., and R. Bugat.** Facteurs génétiques dans le determinisme du cycle veille-sommeil chez la souris. *Brain Res*. 69: 315–330, 1974.
40. **Vanderwolf, C. H.** The electrocorticogram in relation to physiology and behavior: a new analysis. *Electroencephalogr. Clin. Neurophysiol*. 82: 165–175, 1992.
41. **Vertes, R. P.** An analysis of ascending brain stem systems involved in hippocampal synchronization and desynchronization. *J. Neurophysiol*. 46: 1140–1159, 1981.
42. **Vertes, R. P., and B. Kocsis.** Brainstem-diencephalo-septohippocampal systems controlling the theta rhythm of the hippocampus. *Neuroscience* 81: 893–926, 1997.
43. **Vinogradova, O. S.** Expression, control, and probable functional significance of the neuronal theta-rhythm. *Prog. Neurobiol*. 445: 523–583, 1995.
44. **Vogel, F.** *Über die Erblichkeit des normalen Elektroenczephalogramms*. Stuttgart, Germany: Thieme, 1958.
45. **Vogel, F.** The genetic basis of the normal human electroencephalogram (EEG). *Humangenetik* 10: 91–114, 1970.
46. **Webb, W. B., and S. S. Campbell.** Relationships in sleep characteristics of identical and fraternal twins. *Arch. Gen. Psychiatry* 144: 201–204, 1983.
47. **Wimer, R. E., C. C. Wimer, and T. H. Roderick.** Genetic variability in forebrain structures between inbred strains of mice. *Brain Res*. 16: 257–264, 1969.